

# Impulse facilities for the simulation of hypersonic radiating flows

R.G. Morgan, T.J. McIntyre, D.R. Buttsworth, P.A. Jacobs, D.F. Potter,  
A.M. Brandis, R.J. Gollan, C.M. Jacobs, B.R. Capra, M. McGilvray and T. Eichmann  
*Centre for Hypersonics, University of Queensland, St. Lucia, QLD, 4067, Australia*

## I. Introduction

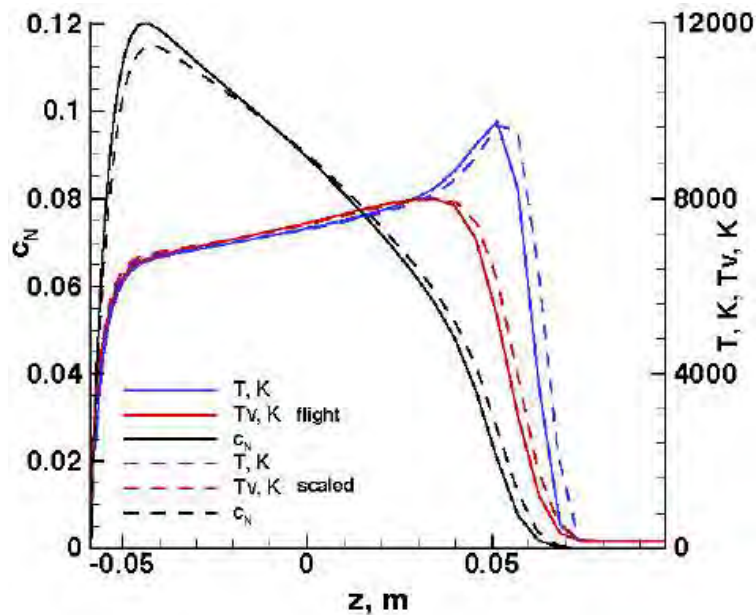
At high flight speeds, radiation becomes an important component of aerodynamic heat transfer, and its coupling with the flow field can significantly change macroscopic features of the flow. As radiating flight conditions are typically encountered in reentry trajectories, the associated flight regimes range from rarefied to continuum, and may have many levels of thermal, chemical and electronic non-equilibrium.

The shock heating of the gas processed by the bow shock of a blunt body at hypervelocity speeds occurs over a distance of several mean free paths, and leaves the gas in a state of chemical and thermal non-equilibrium. In the subsequent relaxation region, non-equilibrium radiation takes place which will have an effect on the total heating to the flight vehicle, to an extent which is determined by the length and density scales involved, and the kinetic properties of the specific species present. The classical wind tunnel technique of studying flight phenomena on small scaled models starts to break down when applied to radiating flows. Provided flight total enthalpy is matched, maintaining the binary scaling parameter in a scaled model may be done by conserving the product of density and a characteristic length scale with flight (commonly referred to as  $\rho$ -L scaling), which conserves Reynolds number and viscous effects, and matches binary chemical processes, such as dissociation. In practice, it can also reproduce more complex reacting schemes surprisingly accurately, as shown by Figure 1, where the reactions from a  $N_2$ - $CH_4$  mixture are well simulated over a scaling length ratio of 100:1.

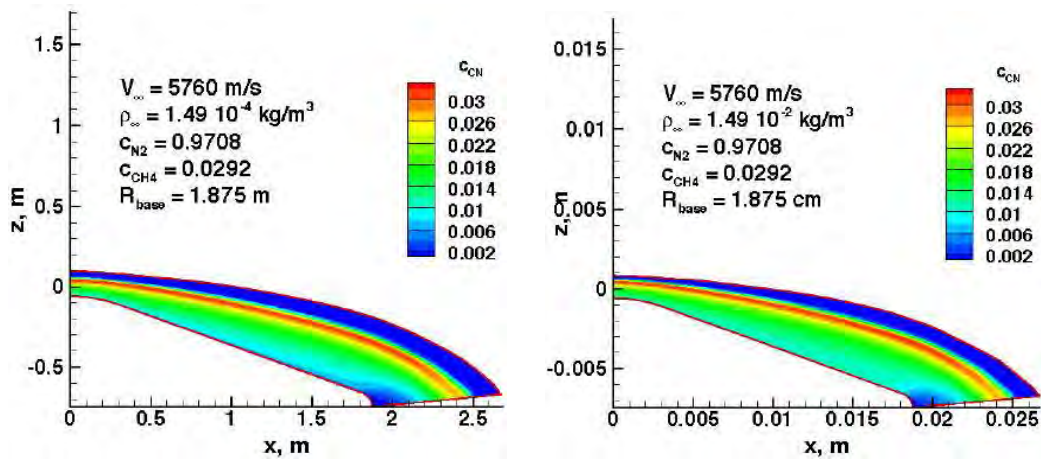
The convective heat transfer is also scaled correctly, and the heat removed from the streamtubes (per unit mass of streamtube flow) will be the same in the scaled and unscaled cases.

However, when the radiation field associated with these two flows is considered, the mathematical similarity breaks down. When the point-to-point transfer of radiation through an optically thin flow is considered, similarity is conserved, because transmission is attenuated in proportion to the exponential of the mass traversed along the line of sight. This scales as the (constant)  $\rho$ -L product. But when the total amount of heat removed from the streamtubes by radiation is considered, that scales in proportion to the volume of gas times a density (ie.  $\rho$ - $L^3$ ), whereas the mass flux into the shock layer scales with the sectional area (ie.  $\rho$ - $L^2$ ). Therefore the amount of heat removed by radiation per unit mass scales in proportion to the absolute length scale. This means that when small scaled models of flight vehicles are tested in the laboratory, not enough heat is removed from the stream tubes by radiation (by an amount equal to the scale factor), and true mathematical similarity is not maintained between tunnel and flight. The significance of this discrepancy will depend on how strong the coupling is between the radiation flux and the aerodynamic flow field. If the total amount of radiated energy is so high that the local thermodynamic condition of the flow is significantly altered (ie it is cooled down), then macroscopic changes to the flow field will occur, and the tunnel will not produce a direct simulation of flight. If the cooling produces only minor changes in condition (ie weak coupling), then the aerothermodynamic flow field is adequately reproduced in the tunnel, and direct simulation of flight will be achieved.

Both these situations are well worth studying experimentally, as they reproduce the physical phenomena which occur in radiating flight, and enable validation of the associated numerical and theoretical modelling. However, it has to be recognised that they do not always provide a direct mathematical simulation for the full flight length scales. Another issue in addition to the lack of coupling, is that it is not fully understood how



(a) Centreline profile



(b) CN concentration - flight

(c) CN concentration - 100:1 scaled

Figure 1: Numerical simulation of flight and expansion tube testing of Titan entry. Calculations by Gnoffo in Morgan et al.<sup>1</sup> (2006).

the fundamental radiation process scales absolutely with pressure. Non equilibrium radiation is basically a rarefied phenomena, associated with insufficient collisions to achieve equilibrium. From a first order analysis relaxation is expected to scale with a  $\rho$ -L product, in proportion to the number of collisions encountered. However, this has not been validated, and molecular size does not scale, and there is still a need to perform experiments at the true densities to be encountered in flight (not those multiplied by 100 as in the example above).

The radiant surface heating component can be very significant, ranging from about 20% of the total for sections of the Apollo return trajectory, 70% for a Titan hard shell aerocapture flight and 95% for a Titan ballute entry, (Cauchon<sup>2</sup> (1967), Wright et al.<sup>3</sup> (2005), Park and Tauber<sup>4</sup> (1999)). The last two numbers are based on unvalidated CFD models, and significant variations on these values are given by different researchers. The 70% value for Titan aerocapture is also in serious doubt, because the data from the EAST facility tests, and the results from recent theoretical modelling. For Titan entry, the main radiating species is CN (cyanogen), the concentration of which can be an order of magnitude above local equilibrium levels in the relaxation zone. The CN is present due to the small quantities of CH<sub>4</sub> in the predominantly N<sub>2</sub> atmosphere. In addition to the chemical non-equilibrium, the population levels of the excited CN states appear to follow a non Boltzman distribution, indicating a fundamental flaw in current modelling procedures, Gnoffo<sup>5</sup> (1999).

To address these issues, more physical data is needed relating to the radiation spectra in the relaxation zone. Whilst there is some flight data available from the FIRE series of flights, Cauchon<sup>2</sup> (1967), flight testing in general is not a viable means of obtaining the comprehensive data involved. The tests are prohibitively expensive and time consuming, and more accurate measurements can be made in a laboratory environment. To address this issue, specific tests have been made in air and N<sub>2</sub>/CH<sub>4</sub> mixtures in the NASA Ames EAST shock tube facility, Bose et al.<sup>6</sup> (2005).

## II. Use of free piston impulse facilities for radiation measurements

Some of the complexities of experimentally validating both the radiation-flow field coupling, and the true high altitude, low density radiating behaviour can be discussed with reference to Figure 2.

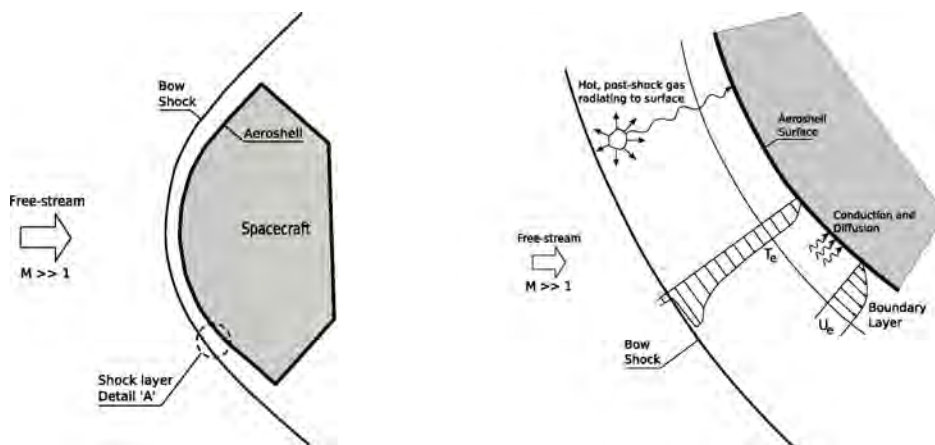


Figure 2: Schematic of radiating shock layers. Taken from Gollan<sup>7</sup> (2008)

To investigate radiation-flow field coupling, the whole flow field surrounding a body has to be simulated, and because spacecraft dimensions are typically in the range of metres, small scale models have to be tested. This requires facilities with very high total pressures and temperatures (typically on the order of GPa and 10s of thousands of Kelvin respectively for superorbital entry). Expansion tubes are the most capable facilities currently available for such study, and this report describes the X1, X2 and X3 family of expansion tubes at The University of Queensland (Morgan<sup>8</sup> (2001)). A schematic of the X2 and X3 free piston facilities can be seen in Figure 3 and 4 with the major dimensions shown. Relevant references on work completed at the University of Queensland on radiation are 1, 7, 9–23.

Experiments performed therein involve coupled radiating flows, but they are not direct simulations of flight conditions, as mentioned above. The coupling of the radiation with the flow will be different, and it is unknown what effect doing the experiments at the higher density required for scaled tests will have on

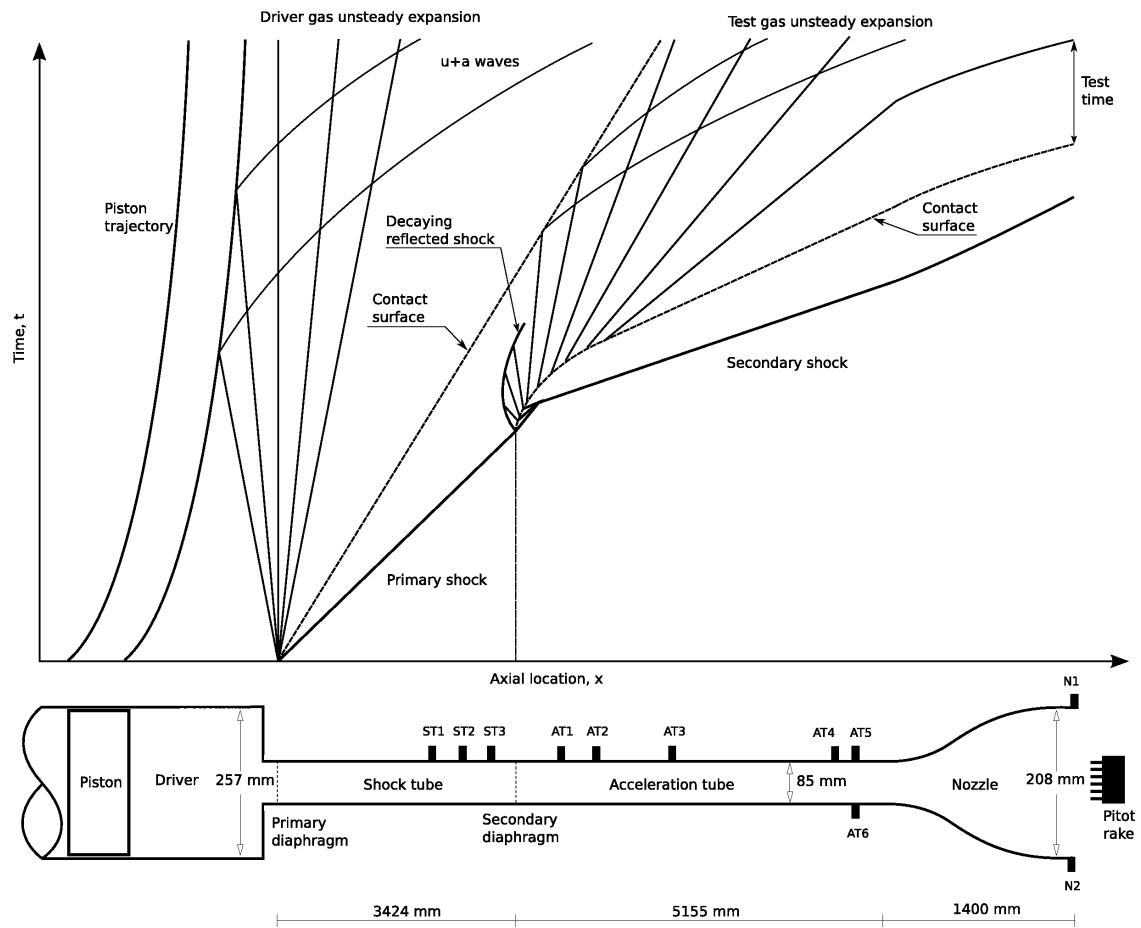


Figure 3: Schematic of X2 in expansion tunnel mode with leading dimensions. Taken from Potter et al.<sup>11</sup> (2008)

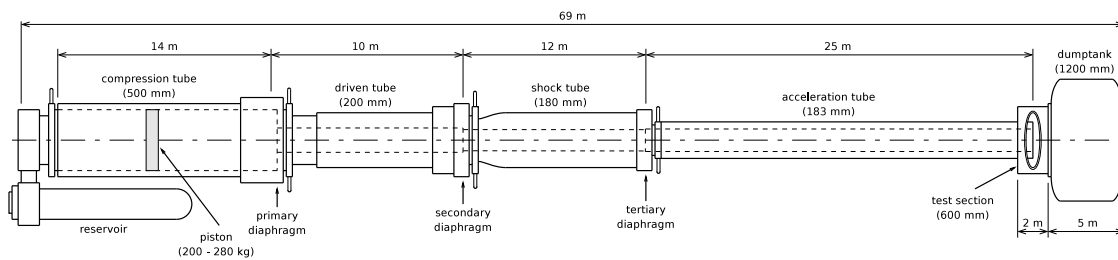


Figure 4: Schematic of X3 expansion tube mode with leading dimensions.

the radiation process. The zones of non-equilibrium radiation are typically of small extent physically, and are located near the bow shock (Figure 1). It is necessary to categorise the appropriate length scales for various missions in order to identify suitable facilities. For the FIRE missions, the shock standoff distance was of the order of 50 mm, with the non-equilibrium zone extending approximately 20 mm behind the shock. For a CEV type lunar return vehicle standoffs of the order of 500 mm are expected, and a Titan hardshell aerocapture capsule would experience standoffs of the order of 200 mm, as indicated by CFD in Figure 2, Gnoffo<sup>5</sup> (1999). For a worst case example, an upper atmosphere Titan ballute vehicle would experience shock standoffs of the order of 1 m, with the non-equilibrium radiation region extending about 300 mm. Typically, therefore, the extent of the non-equilibrium radiation zone will only be in the range of tens to hundreds of mm, at real flight conditions. This opens up the possibility of doing non-reflected shock tunnel (NRT) tests at real flight conditions, but recreating only the flow in the non-equilibrium region, just behind the bow shock.

### III. Non Reflected Shock Tube measurements

In Figure 5, the 2 operating modes are shown. In NRT mode, the flow is examined just after the shock exits the tube, in the region where it is still planar. In the laboratory reference, the flow is unsteady as the shock-discontinuity propagates through the test section. However, as the shock propagates down the tube at a uniform speed, a quasi-steady flow exists in the shock frame of reference. The UQ expansion tubes have been designed with dual-mode configurations, so that they can also do NRT experiments. With the high performance free piston drivers, and the provision for a shock heated intermediate driver tube, they have been used to drive shock at speeds up to 15 km/s, and the exposure times of  $\sim 100$  ns effectively freezes the flow, giving a true comparison of the flow behind a bow shock in flight.

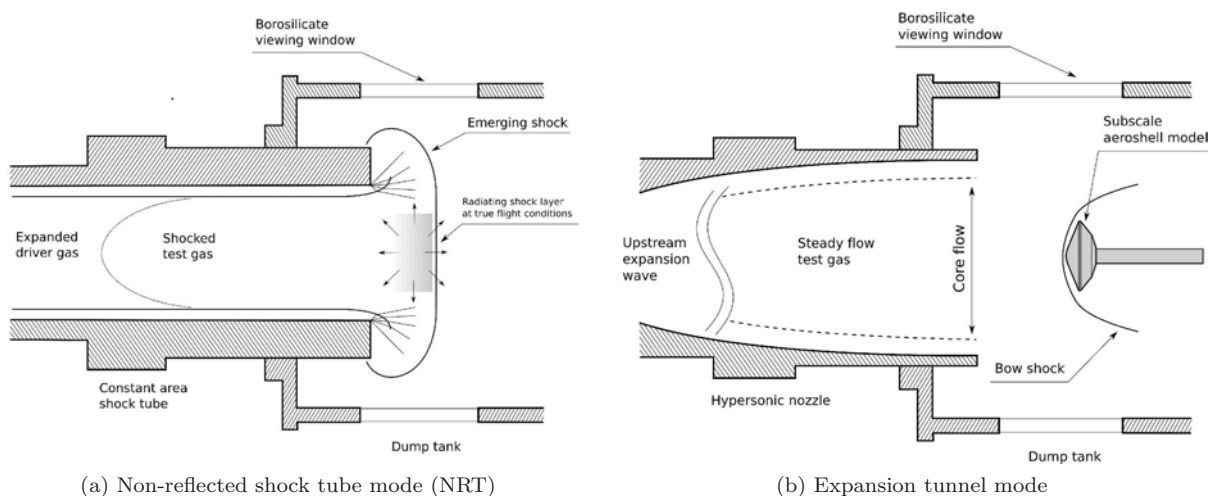


Figure 5: Operational modes for the X-series free piston impulse facilities. Taken from Potter et al.<sup>11</sup> (2008)

The experiments however are non trivial as the densities are so low, containing the flows in a duct such as a shock tube is complicated by the development of thick boundary layers, as shown in Figure 6. This viscous effect is fairly well modelled by the Mirels<sup>24</sup> analysis (1963), and Sharma and Wilson<sup>25</sup> (1996). The net result is that the interface between the driven and driver gases catches up with the shock speed at low densities and long tube lengths, leading to a relatively small slug of shock heated test gas from which radiation measurements can be taken. The effect is increased at high speeds and low densities, and the available slug length scales approximately with the density and with the tube diameter squared, for the laminar boundary layer conditions usually relevant to the low densities involved. It is evident that large bore tubes will be needed to study these effects at high altitudes due to the length required for the non-equilibrium zone.

Sample plots of shock speed against distance are shown in Figure 7 for X3 running in NRT mode at speeds of between 8 and 12 km/s in air. High speeds can be achieved at low density with very little attenuation.

The X2 facility in NRT mode has been used at pressures down to 4 Pa, and still maintained a measurable separation between the shock and driver gas as indicated by high speed photography, pitot measurements

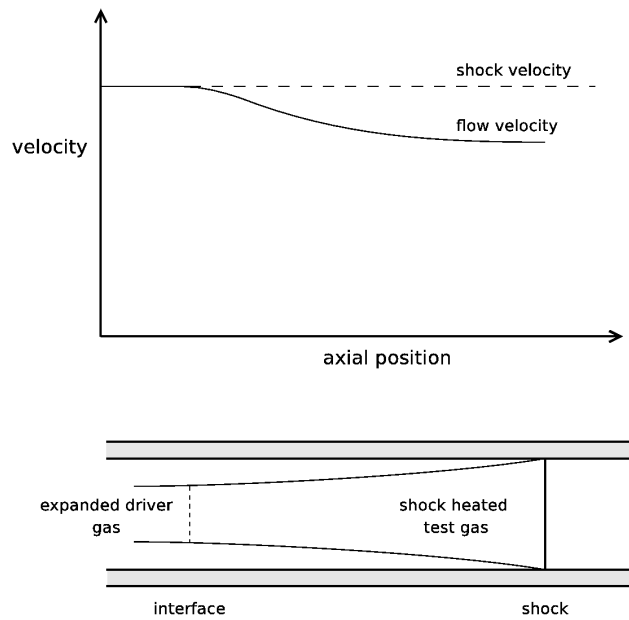


Figure 6: Development of test slug in non-reflected shock tunnel.

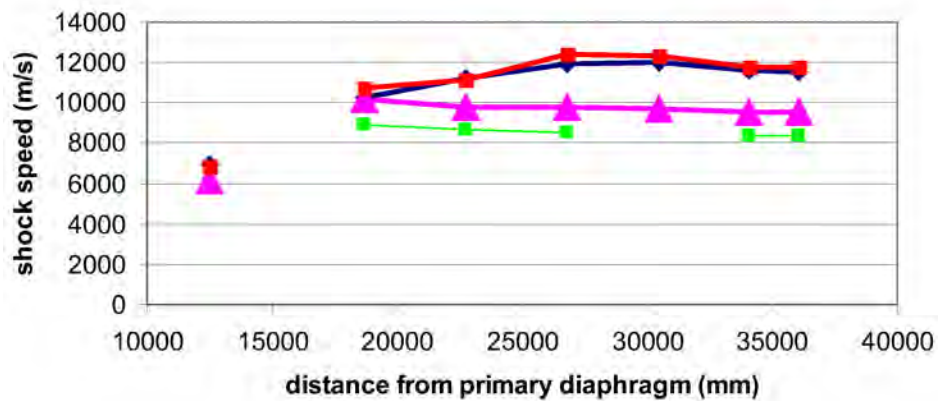


Figure 7: Shock speeds from X3 running in non-reflected shock tube mode. Taken from Morgan et al.<sup>1</sup> (2006)

(Figure 8) and spectrometry. This behaviour has also been noted in axisymmetric calculations of the tunnel flow (Figure 9 and 10), where the shock is relatively planar close to the tube exit. A parametric series of tests has just been completed of 250 shots using  $N_2$ - $CH_4$  mixtures of between 2 and 8.6%  $CH_4$ , speeds of between 4 km/s and 10.5 km/s, and pressures between 1000 Pa and 2 Pa. No measurable flow between shock and driver gas contact surface was found for fill pressures of less than 4 Pa. Absolute calibration of the radiated flux was obtained, though it has not yet been processed for all shots. X3 has been used to generate flows at higher velocities and lower densities, but spectrometric measurements have not been recorded in it yet.

Noting the dependency of test slug length on the square of diameter, it is expected that the X3 facility (with a diameter of 183 mm compared to 85 mm for X2) will be able to generate useful radiating flows at pressures down to the order of 1 Pa, at speeds of the order of 10 km/s. We have also fabricated a new section for X2, made of Aluminium and with an internal diameter of 155 mm. This should enable the operating envelope to extend downwards in pressure to  $\sim 1$  or 2 Pa. Once these measurements have been successfully taken and validated, there is the possibility of expanding the diameter of the X3 driven tube further, to 500 mm. This in theory would allow shocks at pressures of  $\sim 0.1$  Pa to be studied, with shock

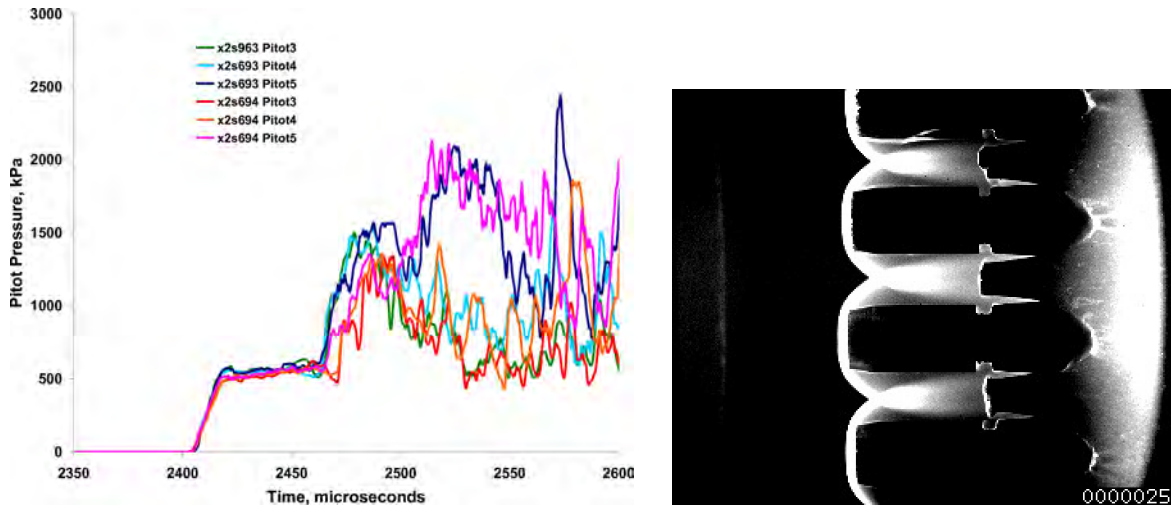


Figure 8: Sample Pitot traces for two repeat shots (133 Pa, 98% N<sub>2</sub> / 2% CH<sub>4</sub>, 5.7 km/s) in X2 configured as NRT. Three transducers on each run spaced 35 mm apart each, symmetrically spaced and Located at axial station 25 mm from tube exit, demonstrating repeatability and uniformity. Steady flow is indicated by level region on left, driver gas arrival and flow termination shown by the sudden rise in pressure after 50 μs.

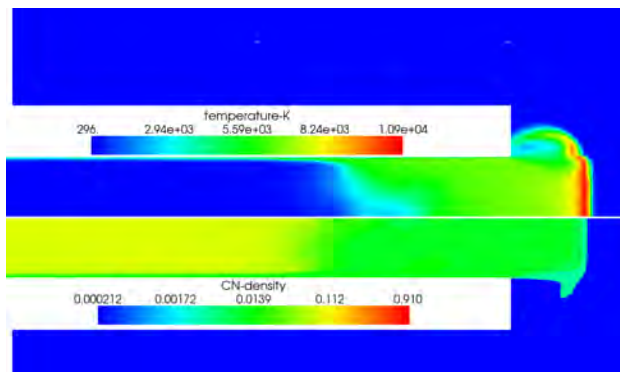


Figure 9: CFD of flow leaving X2 in non-reflected shock tube mode for a Titan condition. Taken from Gollan et al.<sup>12</sup> (2007)

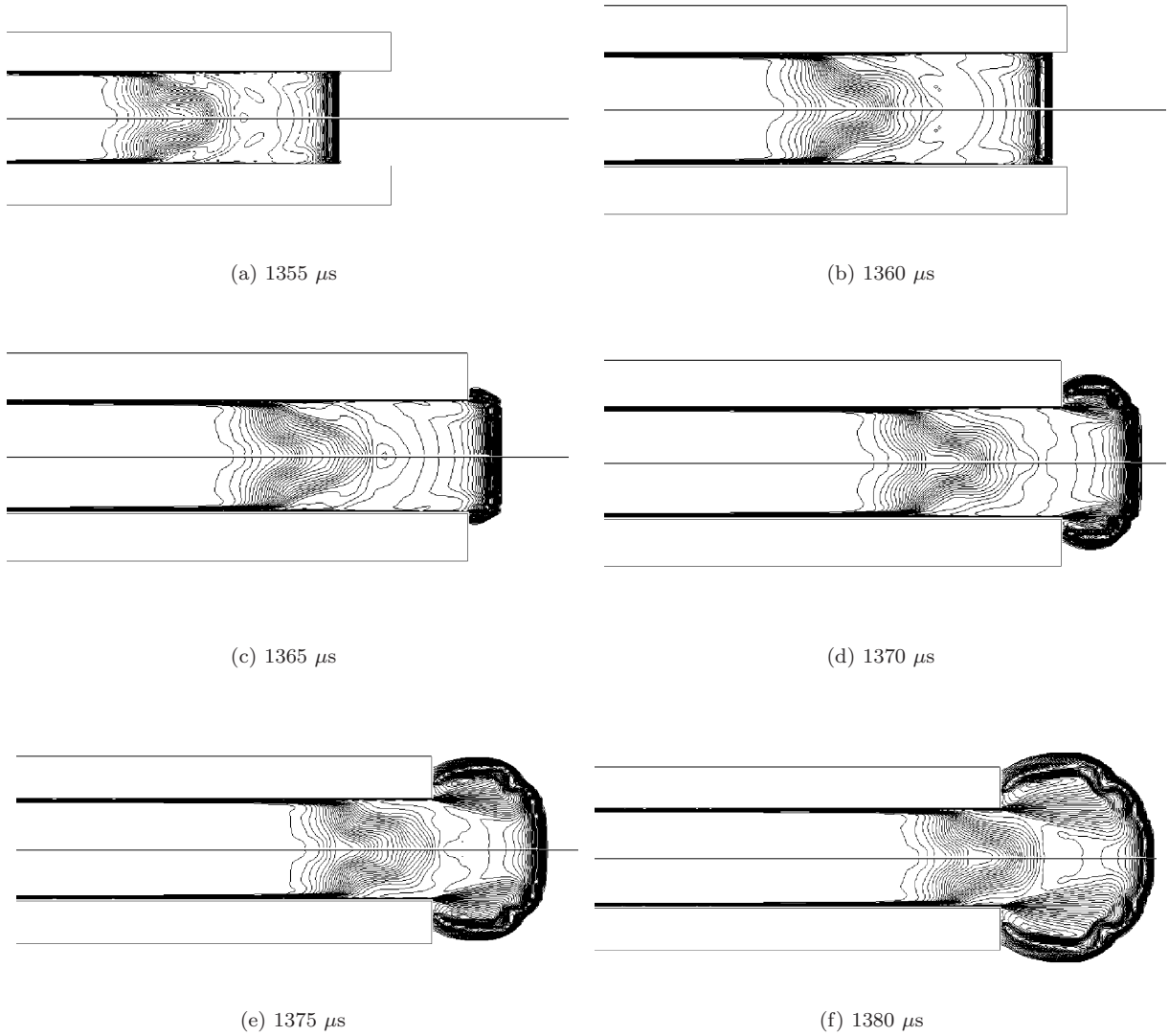


Figure 10: Development of shock into test section, showing planar region. Taken from Gollan<sup>7</sup> (2008)

interface separations of  $\sim 200$  mm, which probably represents the lowest values really needed (for, say, the reproduction of the radiation layer around a Titan upper atmosphere entry deployable ballute). In principle, the facility could drive tubes of up to 1500 mm in diameter at similar speeds due to the high performance free piston and shock heated driver combination, but there are no missions anticipated at present which would demand such conditions.

### III.A. Geometric similarity for correctly coupled flows

The radiating zone behind the normal shock will be the same size in the flow direction as in flight, if the tests are performed at true flight density. However, as mentioned above the full aerodynamic flow field is not reproduced, and in particular, the curved bow shock from flight is replaced by a normal shock in the test section. If shock curvature can be assumed negligible (i.e. the shock radius of the curvature is typically is much larger than the radiating zone and the shock layer), then the tunnel measurements can be used to estimate the surface heat flux which would be expected in flight.

Noting that in the laboratory, the radiating layer is probed from the side (in the plane of the layer), and in flight, the radiation is received in a direction perpendicular to the source plane, corrections can be made for different optical path lengths and solid angles. In this way, direct simulation of the radiant heat source flux in flight becomes possible, including the coupling radiation with the flow properties (for a very small section of the overall flow field). A geometric error is introduced due to shock curvature, which would appear to be equivalent to the tangent-slab approximation commonly made in numerical simulation of the radiation flux.

A possible alternative to this approach is to use the expanding shock wave in the dump tank, downstream from the tunnel exit. The state of the flow of interest can be seen in Figure 10f, whereby this stage, the shock wave has a significant radius of curvature. If an appropriate axial location from the tube exit was chosen, the radius of curvature could be matched to a specific flight geometry. In this way, a small section of the aerodynamics around a capsule could be simulated for real flight conditions. A schematic of this process can be seen in Figure 11. It should be noted that the expanding shock formation is an unsteady process, which attenuates as it propagates away from the source, so its direct comparison to steady flight is not yet proven. Also, the curved shock around a flight vehicle is formed from the locus of a family of oblique shocks, all with a constant free stream speed and direction (Figure 11a). In the expanding shock tube flow, the curved shock is actually the locus of a series of normal shocks, each with a slightly different direction of propagation (Figure 11b). When the laboratory reference frame is transformed to a quasi-steady shock fixed reference on the centre line, minor distortion of the off-axis flow field will occur. It is currently being investigated whether the effect of the transient terms are much larger than the steady state fluxes, and a similarity with flight can be demonstrated with correct geometrical and radiative coupling.

### III.B. Imaging capabilities for radiating flows

Spectral imaging is achieved using an intensified CCD camera (Princeton Instruments PI-MAX) coupled to an imaging spectrograph (Acton Research Spectra Pro SP2300 series). The group has two complete systems, one capable of imaging over the wavelength range of 200-600 nm, while the other is sensitive over the range 400-800 nm. The images obtained with these systems consist of a two-dimensional distribution of intensity; one dimension is spectral while the other dimension is spatial (aligned along the entrance slit of the spectrometer).

The systems are calibrated using an Optronic Laboratories OL-200M standard of spectral irradiance. The lamp is placed to generate a known spectral irradiance in the test section and then the light is imaged through the optical system to determine the sensitivity of the camera.

The resolution of each system is dependent on the operation mode. To probe the radiation from aerodynamic flows over blunt bodies, an imaging system is established that records the radiation along the stagnation streamline in front of the body. In a recent study of flow over a cylinder, the imaged region was around 5 mm long (covering 256 pixels on the camera) by about 100  $\mu\text{m}$  high (as set by the entrance slit of the spectrometer). For non-reflected shock tube tests, a larger region, some 80 mm long by 1 mm high has been imaged.

The spectral resolution is controlled by varying the size of the input slit to the spectrometer and by using one of three available interchangeable gratings. The gratings give single shot wavelength ranges across the 1024 pixels of the camera of about 40 nm, 120 nm and 480 nm. The sensing elements of the ICCD camera

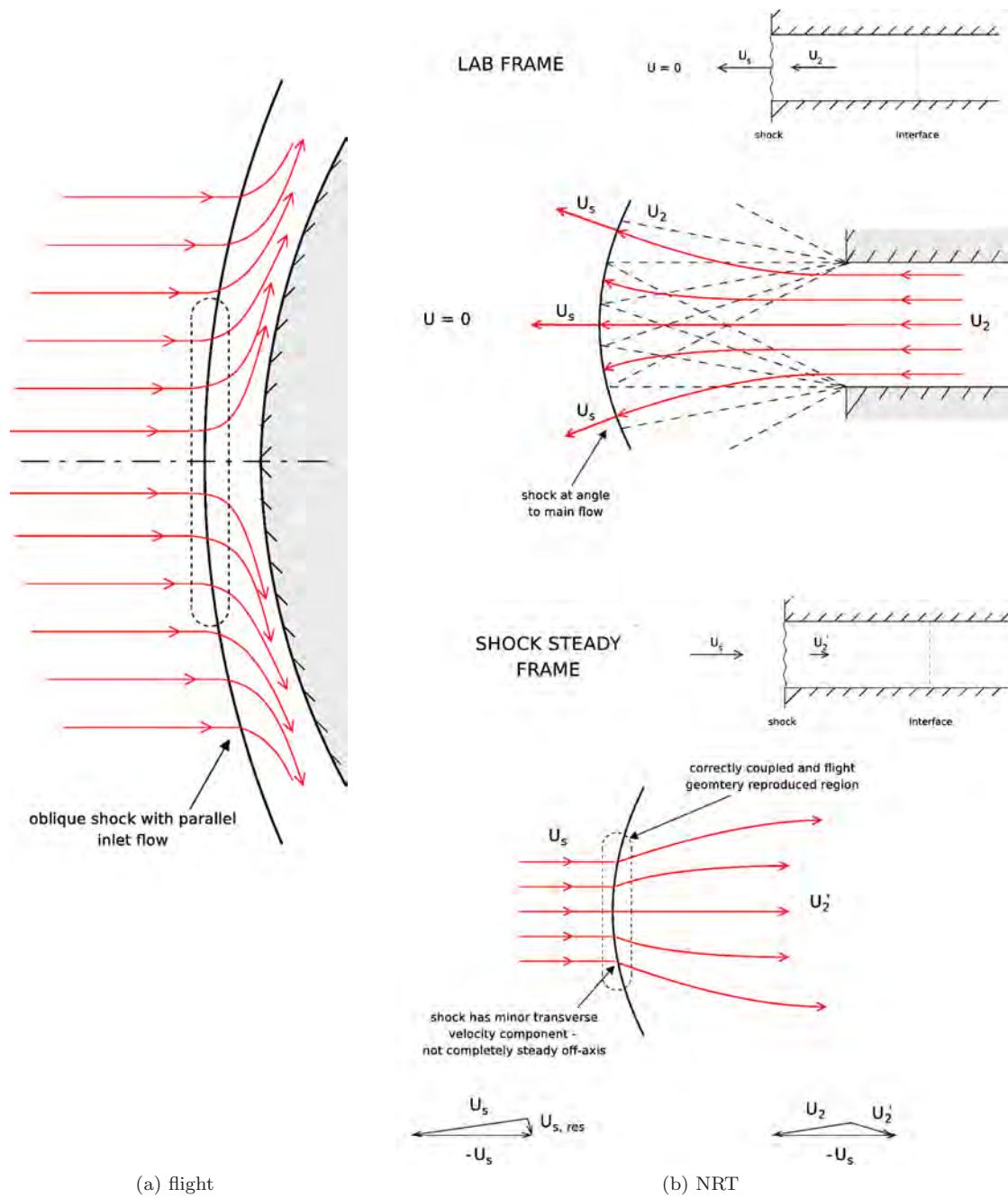


Figure 11: Schematic of the use of shock curvature in NRT to reproduce geometry and radiation where a significant radius of curvature is present.

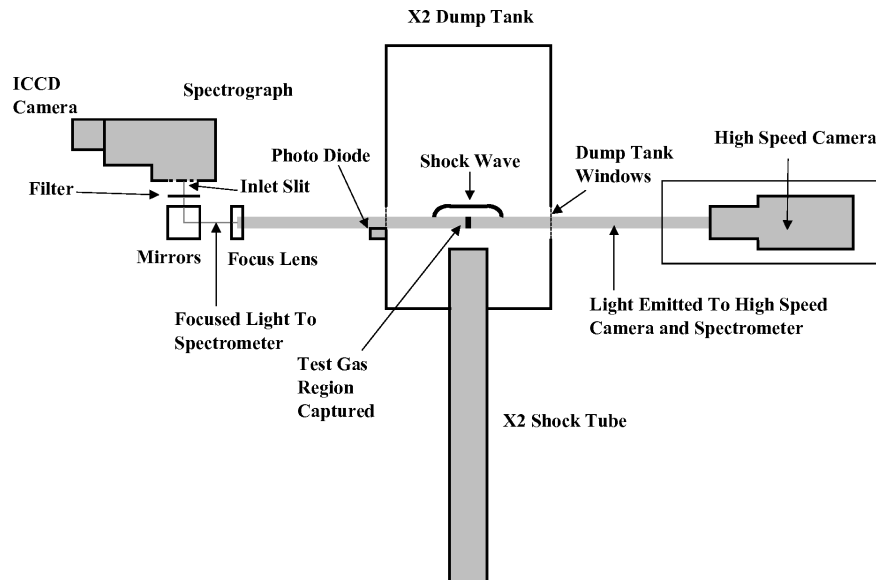


Figure 12: Experimental arrangement for the spectral imaging in X2. Taken from Brandis et al.<sup>10</sup> (2008)

are 16 bit resolution. The sensitivity of the system is dependent on the size of the area imaged, the spectral resolution, and the capturing optics utilised in the imaging. To give an indication of the system capabilities, Figure 13 shows preliminary results of spectra recorded in non-reflected shock tube mode.

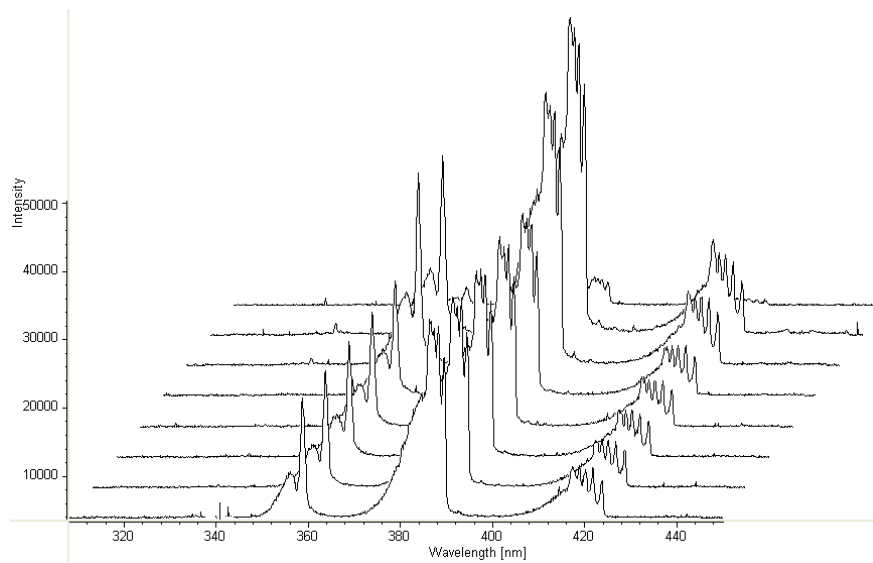


Figure 13: Wavelength profiles at different axial locations for Titan shot in NRT. Taken from Brandis et al.<sup>10</sup> (2008)

Brandis et al.<sup>10</sup> visualised the shock for a Titan condition as it exited the tube, using a 1 MHz Shimadzu Hyper Vision HPV 1 high speed camera. The flat shape of the shock in the field of view, the thickness of the strongly radiating region behind the shock and the termination of radiation on driver gas arrival are all consistent with the pitot pressure measurements, the spectroscopic record, and the CFD (Figure 10).

## IV. Expansion tube mode

### IV.A. Direct imaging of coupled flow field

An example of simulating a coupled flow field is shown in Figure 14. The model is a 25 mm diameter cylinder 102 mm long, orientated normal to the flow. A steady shock layer flow is established, and spectrometry is used to quantify the radiation field along the stagnation streamline. The test gas is 4% CO<sub>2</sub> in N<sub>2</sub>, at a total enthalpy of 24.7 MJ/kg. Comparison of CFD with the tunnel operation showed good agreement with the measured levels of pitot and static pressures (Figure 15). CFD analysis with and without radiation coupling showed that the flow was coupled, through changes to the shock standoff, which was an easy parameter to measure experimentally. Sample spectra are shown in Figure 16, and show significant departures in profile from a simple prediction.

This experiment demonstrates the use of full aerodynamic flow simulation of a coupled radiating flow field, for the purposes of validating coupled codes, and for testing the detailed radiation models developed with non-reflected shock tube experiments in a full flow situation. As mentioned above, the expansion tube flow will not relate exactly to any real (larger scale) flight condition, but the codes, when validated, may then be used to analyse the full flight length scales.

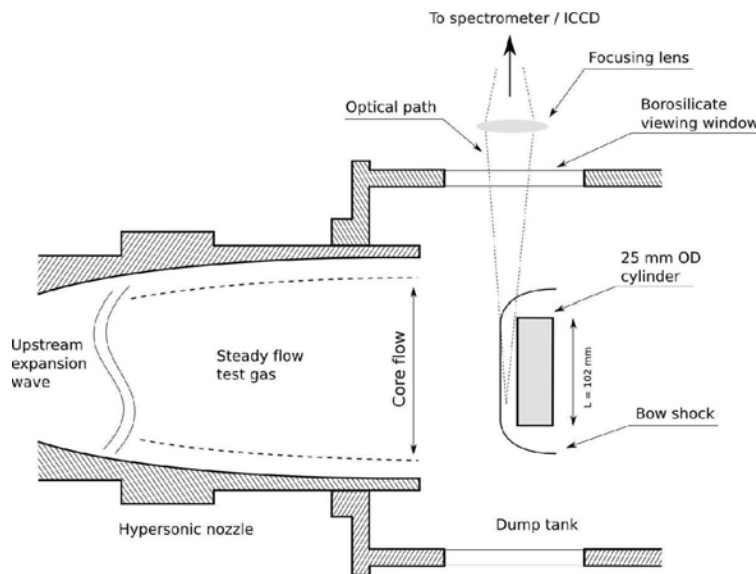


Figure 14: Schematic of cylinder simulated in expansion tunnel with coupled flow. Taken from Potter et al.<sup>11</sup> (2008)

### IV.B. Instrumentation for bulk radiation measurements

The spectral measurements discussed above are very useful for understanding the physical processes involved in radiating flows, and for validating numerical codes for coupled flow. However, it is also very useful for engineering purposes to have the capability for direct measurement of total radiation, and the separation of the radiant component. With this in mind, bulk radiation gauges have been developed at UQ, which measure the radiation from behind a glass window set into the windward model surface. Simultaneously, total heat transfer is measured by an external thermocouple gauge so that the ratio of radiant to convective heat transfer can be measured directly. These are used in expansion tube mode, with  $\rho$ -L scaling. As a demonstration, they were used by Capra<sup>13</sup> (2007), on a Titan aerocapture model with Pathfinder sphere-cone geometry, using 5% CH<sub>4</sub> in N<sub>2</sub>.

The construction is shown in Figure 17, and they consisted of thin film gauges behind a glass window. Sample data is shown below (Figure 18 and 19), and compared to various numerical predictions, with appropriate scaling. It is interesting to note that the experimental measurements are all well below the numerical predictions, even with coupling, giving another indication that more work is still needed in the modelling field.

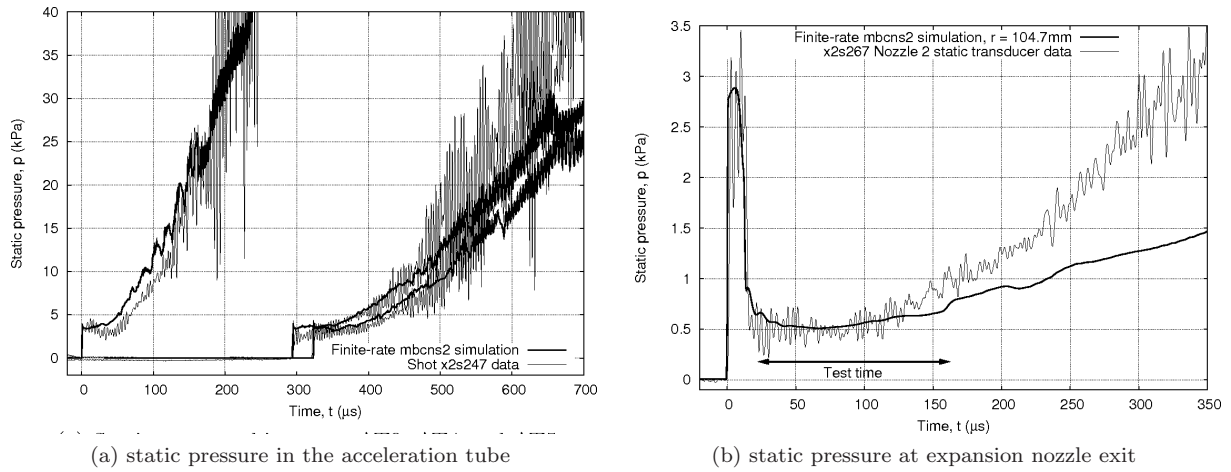


Figure 15: Comparison of expansion tunnel flow measurements with CFD of facility. Taken from Potter et al.<sup>11</sup> (2008)

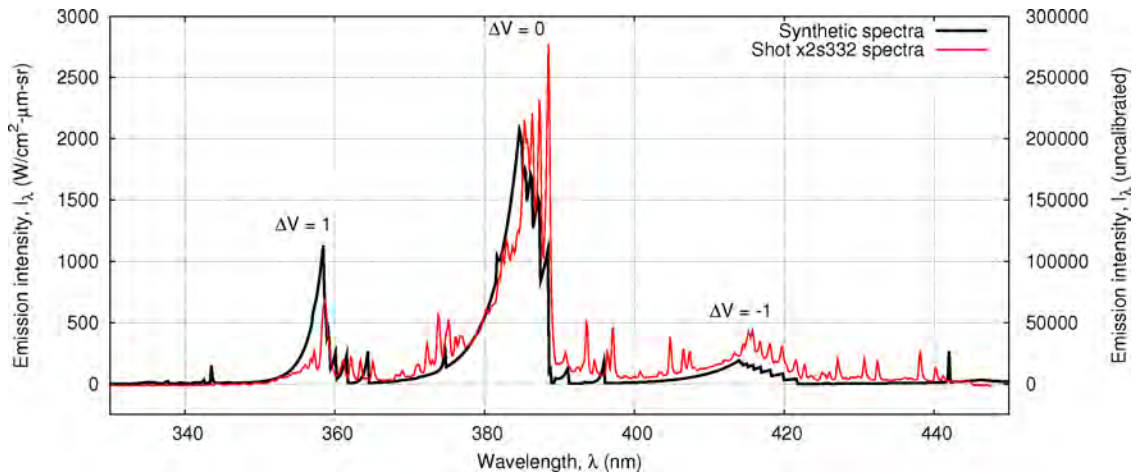


Figure 16: Peak emission of spectra 0.329 mm behind the shock for a radiatively coupled cylinder simulation. Taken from Potter et al.<sup>11</sup> (2008)

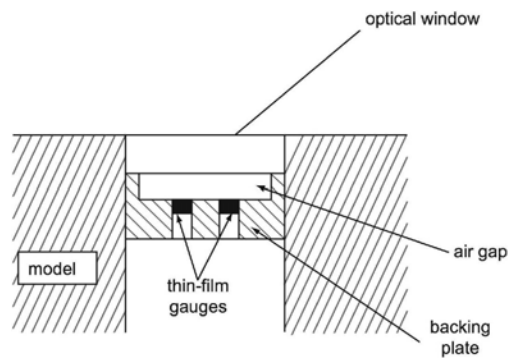


Figure 17: Bulk radiation measurement gauge. Taken from Capra et al.<sup>9</sup> (2004)

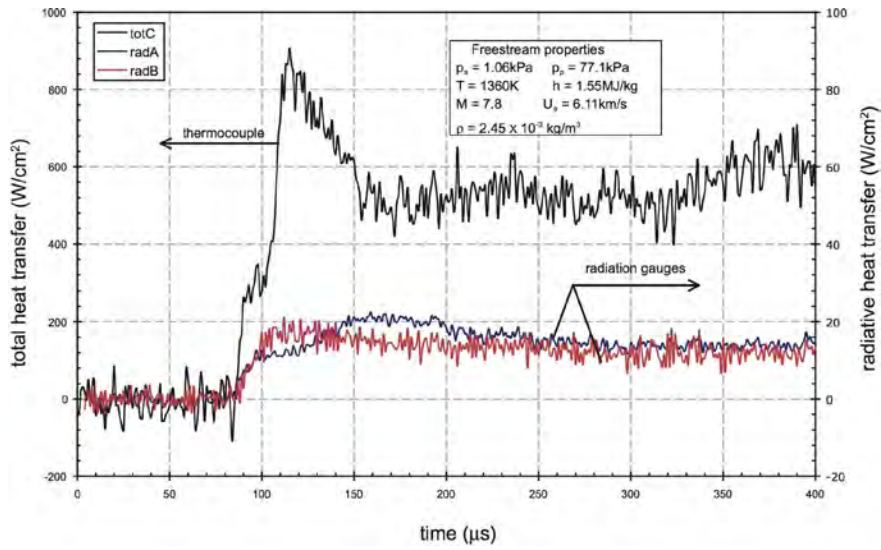


Figure 18: Comparison of total and radiant heat flux. Taken from Capra<sup>13</sup> (2007)

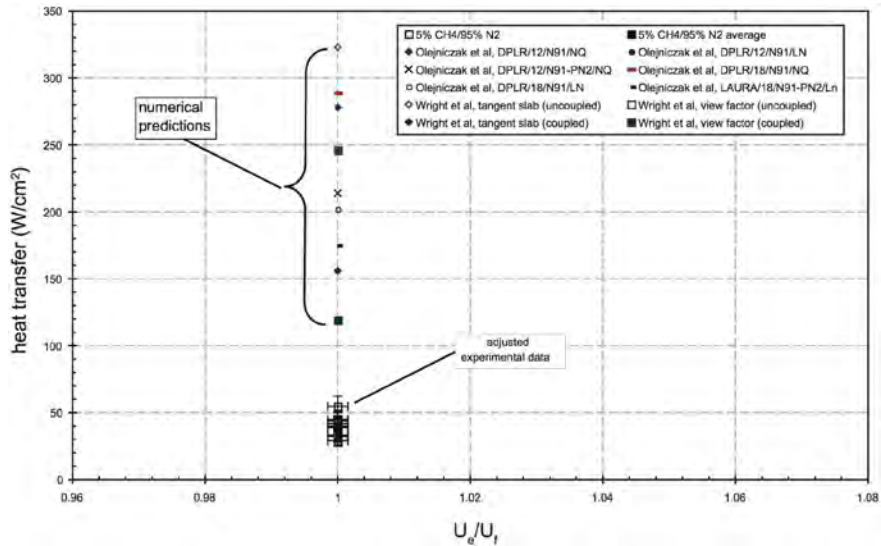


Figure 19: Comparison of expansion tube measurements with various numerical predictions. Taken from Capra<sup>13</sup> (2007)

By looking through a glass window, the vacuum ultra-violet radiation is precluded, which is not so important for the Titan atmosphere, but cuts out an important part of the spectrum for air and CO<sub>2</sub> atmospheres. A further version of the bulk radiation gauge is currently under development, whereby the sensor looks at the flow from behind a layer of helium, rather than glass. The helium is introduced into a cavity in front of the sensor by injection at a pressure slightly higher than pitot, fractionally before the flow arrives. The layer of helium then protects the sensor from the convective heating on the external surface, but allows the radiation to pass through. With suitable calibration and analysis, quantitative measurements of the surface radiant heat flux can be obtained. The schematic is shown in Figure 20. A prototype has been tested in X2, but is not yet proven to be effective. If the concept can be made to work reliably, it will be a useful piece of instrumentation for investigating flows with strong vuv radiation.

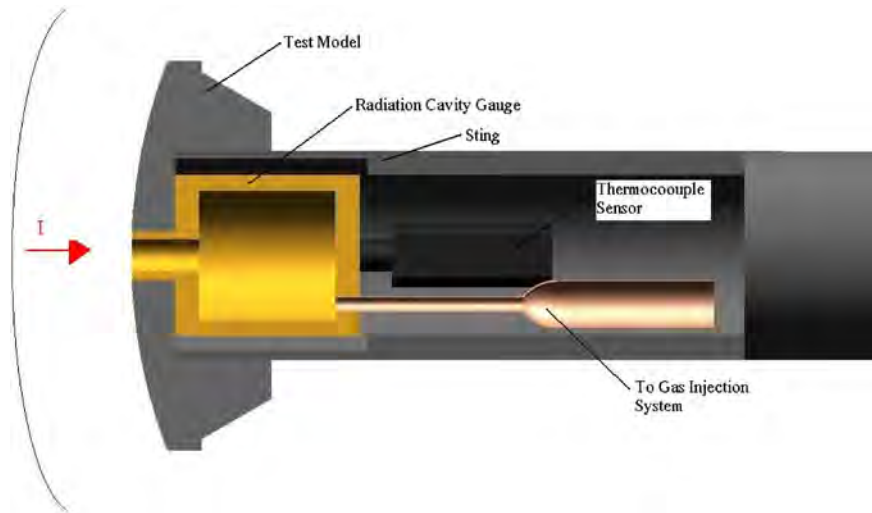


Figure 20: Helium screened radiation gauge. Taken from Capra<sup>13</sup> (2007)

## V. Conclusion

By use of a combination of non-reflected shock tube and expansion tube facilities, a range of radiative phenomenon relating to hypervelocity flight can be investigated. This will enable the validations of fundamental modelling of the radiative processes, and the coupling of those high speed processes with the aero-thermodynamics of flight.

## VI. Acknowledgements

This work was supported by the Australian Research Council (ARC).

## References

- <sup>1</sup>R. Morgan, T. McIntyre, R. Gollan, P. Jacobs, A. Brandis, M. McGilvray, D. van Diem, P. Gnoffo, M. Pulsonetti, and M. Wright. Radiation measurements in non reflected shock tunnels. *36th AIAA Fluid Dynamics Conference and Exhibit*, San Francisco, AIAA 2006-2958, June 2006.
- <sup>2</sup>D.L. Cauchon. Radiative heating results from the fire ii flight experiment at a reentry velocity of 11.4 kilometers per second. *NASA TM X-1402*, July 1967.
- <sup>3</sup>M.J. Wright, D. Bose, and J. Olejniczak. Impact of flowfield radiation coupling on aeroheating for titan aerocapture. *AIAA Journal of Thermophysics and Heat Transfer*, 19(1), 2005.
- <sup>4</sup>C. Park and M. Tauber. Heatshielding problems, a review. *30th AIAA Fluid Dynamics Conference, Norfolk, Va*, AIAA Paper 99-3415, 1999.
- <sup>5</sup>P.A. Gnoffo. Planetary-entry gas dynamics. *Annual Review of Fluid Mechanics*, 31:459–494, 1999.
- <sup>6</sup>D. Bose, M.J. Wright, W.D. Bogdanoff, G.A. Raiche, and G.A. Allen. Modeling and experimental validation of cn radiation behind a strong shock wave. *43rd AIAA Aerospace Science Meeting and Exhibit*, AIAA Paper 2005-0768, 2005.
- <sup>7</sup>R.J. Gollan. *The Computational Modelling of High-Temperature Gas Effects with Application to Hypersonic Flows*. PhD thesis, University of Queensland, St. Lucia, Australia (to be submitted/examined), 2008.

<sup>8</sup>R.G. Morgan. *Handbook of Shock Waves*, eds Ben-Dor, G., Igra, O. and Elperin, T., volume 1, chapter 4.3: Shock Tubes and Tunnels: Facilities, Instrumentation, and Techniques, Free Piston Driven Expansion Tubes, pages 603–622. Academic Press, San Diego, 2001.

<sup>9</sup>B.R. Capra, R. G. Morgan, and P. Leyland. New gauge design to measure radiative heat transfer to a titan aerocapture vehicle in expansion tubes. *Proceedings of the Fifth European Symposium on Aerothermodynamics for Space Vehicles*, ESA SP-563, 2004.

<sup>10</sup>A.M. Brandis, R.G. Morgan, C.O. Laux, T. Magin, T.J. McIntyre, and P.A. Jacobs. Nonequilibrium radiation measurements and modelling relevant to titan entry. *AIAA Journal of Thermophysics and Heat Transfer*, (to be submitted), 2008.

<sup>11</sup>D.F. Potter, R.J. Gollan, T. Eichmann, T.J. McIntyre, R.G. Morgan, and P.A. Jacobs. Simulation of CO<sub>2</sub>-N<sub>2</sub> expansion tunnel flows for the study of radiating shock layer. *AIAA Aerospace Sciences Meeting, Reno, Nevada*, January 2008.

<sup>12</sup>R.J. Gollan, C.M. Jacobs, P.A. Jacobs, R.G. Morgan, T.J. McIntyre, M.N. Macrossan, D.R. Buttsworth, T.N. Eichmann, and D.F. Potter. A simulation technique for radiating shock tube flows. *Proceedings of the 26th International Symposium on Shock Waves, Goettingen, Germany*, July 2007.

<sup>13</sup>B.R. Capra. *Aerothermodynamic simulation of subscale models of the FIRE II and Titan Explorer vehicles in expansion tubes*. PhD thesis, University of Queensland, St. Lucia, Australia, 2007.

<sup>14</sup>B.R. Capra, P. Leyland, and R.G. Morgan. Subscale testing of the fire ii vehicle in a superorbital expansion tube. *42nd AIAA Aerospace Sciences Meeting and Exhibit*, AIAA Paper 2004-1298, 2004.

<sup>15</sup>B.R. Capra, , and R.G. Morgan. Radiative and total heat transfer measurements to a titan explorer model. *4th AIAA/AHI Space Planes and Hypersonic Systems and Technologies Conference*, 2006.

<sup>16</sup>P. A. Jacobs, T. B. Silvester, R. G. Morgan, M. P. Scott, R. J. Gollan, and T. J. McIntyre. Super-orbital expansion tube operation: Estimates of flow conditions via numerical simulation. *43rd AIAA Aerospace Sciences Meeting*, AIAA paper 2005-694, January 2005.

<sup>17</sup>P.A. Jacobs. MB.CNS: A computer program for the simulation of transient compressible flow. Departmental Report 10/96, Department of Mechanical Engineering, University of Queensland, St. Lucia, Qld 4072., 1996.

<sup>18</sup>P.A. Jacobs. Shock tube modelling with L1d. Departmental Report 13/98, Department of Mechanical Engineering, University of Queensland, St. Lucia Qld 4072., 1998.

<sup>19</sup>A.M. Brandis, R.J. Gollan, M.P. Scott, R.G. Morgan, P.A. Jacobs, and P.A. Gnoffo. Expansion tube operating conditions for studying nonequilibrium radiation relevant to titan aerocapture. *42nd Joint Propulsion Conference and Exhibit*, AIAA Paper 2006-4517, July 2006.

<sup>20</sup>T.J. McIntyre, A.I. Bishop, H. Rubinsztein-Dunlop, and P.A. Gnoffo. Experimental and numerical studies of ionizing flow in a super-orbital expansion tube. *AIAA Journal*, 41(11):2157–2161, 2003.

<sup>21</sup>T.J. McIntyre, M.J. Wegener, A.I. Bishop, and H. Rubinsztein-Dunlop. Simultaneous twowavelength holographic interferometry in a superorbital expansion tube facility. *Applied Optics*, 36:8128–8134, 1997.

<sup>22</sup>A.J. Neely and R.J. Morgan. The superorbital expansion tube concept, experiment and analysis. *The Aeronautical Journal*, 98:97–105, 1994.

<sup>23</sup>M.P. Scott, P.A. Jacobs, and R.G. Morgan. Nozzle development for an expansion tunnel. *4th International Symposium on Shock Waves, Beijing, China*, July 2004.

<sup>24</sup>H. Mirels. Test time in low-pressure shock tubes. *The Physics of Fluids*, 6(9):1201–1214, 1963.

<sup>25</sup>S.P. Sharma and G.J. Wilson. Computations of axisymmetric flows in hypersonic shock tubes. *AIAA Journal of Thermophysics and Heat Transfer*, 10(1):169–176, 1996.